Molecular Crystals and Liquid Crystals

Publication details, including instructions for authors and subscription information:
http://www.tandfonline.com/loi/gmcl20

Dielectric Properties of Strongly Polar Nematogens with Cyano and Fluoro Substituents

Joanna Czub [a], Stanisław Urban [a], Dorota Ziobro [b] & Roman Dąbrowski [b]

[a] Institute of Physics, Jagiellonian University, Reymonta, Krakow, Poland

[b] Institute of Chemistry, Military University of Technology, Warsaw, Poland

Version of record first published: 05 Oct 2009

To cite this article: Joanna Czub, Stanisław Urban, Dorota Ziobro & Roman Dąbrowski (2009): Dielectric Properties of Strongly Polar Nematogens with Cyano and Fluoro Substituents, Molecular Crystals and Liquid Crystals, 508:1, 286/[648]-295/[657]

To link to this article: http://dx.doi.org/10.1080/15421400903065762

Mol. Cryst. Liq. Cryst., Vol. 508, pp. 286/[648]–295/[657], 2009

ISSN: 1542-1406 print/1563-5287 online
DOI: 10.1080/15421400903065762

Dielectric Properties of Strongly Polar Nematogens with Cyano and Fluoro Substituents

Joanna Czub[1], Stanisław Urban[1], Dorota Ziobro[2], and Roman Dąbrowski[2]
[1]Institute of Physics, Jagiellonian University, Reymonta, Krakow, Poland
[2]Institute of Chemistry, Military University of Technology, Warsaw, Poland

Dielectric properties of several compounds with cyano and fluoro substituents were studied in the frequency range of 1 kHz – 3 GHz. Most of compounds exhibit nematic mesophase in a broad temperature range. The principal permittivity components and the relaxation processes were studied in the isotropic and the nematic phases. The dipole structure of molecules was analysed. The relaxation times and the activation barriers characterizing the principal molecular motions were determined. The substances show strong dependence of the dielectric anisotropy upon frequency: it changes its sign at high frequencies. Such compounds are useful to formulation of nematic mixtures for double frequency addressing system.

Keywords: dielectric properties; dipole moment; liquid crystals

1. INTRODUCTION

Strongly polar liquid crystal (LC) substances are very important for application purposes. They are widely used while preparing mixtures in order to achieve desirable values of the permittivity tensor components. Consequently, determination of the dielectric properties of pure components is indispensable for composing the mixture.

The aim of this work was to analyse the influence of the dipole structure of eight LC compounds with cyano and fluoro substituents on their dielectric properties. All substances show the nematic (N) polymorphism. Additionally, one of the compounds exhibits the monotropic

Address correspondence to Dr. Joanna Czub, Institute of Physics, Jagiellonian University, Reymonta 4, Krakow 30-059, Poland. E-mail: joanna.czub@uj.edu.pl

smectic A (S_A) phase. The dielectric properties in the LC and the isotropic phase were studied in dependence of temperature and frequency.

The following parameters were studied: the permittivity components $\varepsilon_{||}$ and $\varepsilon_{\perp}$ as a function of temperature and frequency, the dielectric anisotropy $\Delta\varepsilon = \varepsilon_{||} - \varepsilon_{\perp}$ at low (static) and high frequencies, the crossover frequency f_{co} at which the dielectric anisotropy changes its sign, the dielectric relaxation time $\tau_{||}$ for the end-over-end molecular rotation in the LC phases and the activation enthalpy ΔH hindering this motion. The results are discussed as related to the dipole structure of molecules.

2. EXPERIMENTAL

All compounds were synthesised in the Institute of Chemistry, Military University of Technology, Warsaw, according to the route described in [1]. Their chemical formulas and the transitions temperatures are presented in Table 1.

Dielectric measurements were performed with the aid of a HP 4192A impedance analyser in the frequency range of 10 kHz – 20 MHz in the LC phases and a time domain spectrometer (TDS) in the frequency range of 10 MHz – 3 GHz [2] in the isotropic phase. The samples in the N phase were oriented with the magnetic field of 0.8 T. Two experimental geometries were applied: $\mathbf{E}$ II $\mathbf{B}$ and $\mathbf{E} \perp \mathbf{B}$, which enables measurements of two permittivity tensor components, ε_{II} and $\varepsilon_{\perp}$, respectively. The thickness of the sample in the parallel plate capacitor was 0.7 mm. Temperature was stabilized with accuracy of 0.2 K. All measurements were carried out while decreasing temperature which enables supercooling of the LC phases. The highest available temperature was $+160^{\circ}$C.

3. RESULTS AND DISCUSSION

Figures 1 and 2 present comparisons of the dielectric data obtained for the compounds having different chemical structure. Several other parameters, such as values of the permittivity tensor components ε_{II} and $\varepsilon_{\perp}$ taken at the melting point and the dielectric anisotropy values $\Delta\varepsilon = \varepsilon_{||} - \varepsilon_{\perp}$ at low and high frequencies, are listed in the right part of Table 1.

For two substances, (4) and (5), the values of the static permittivity components (especially ε_{II}) are enormously large (see Fig. 1). This is certainly caused by a pronounced conductivity of the substances. In order to estimate true values of the permittivities the measurements

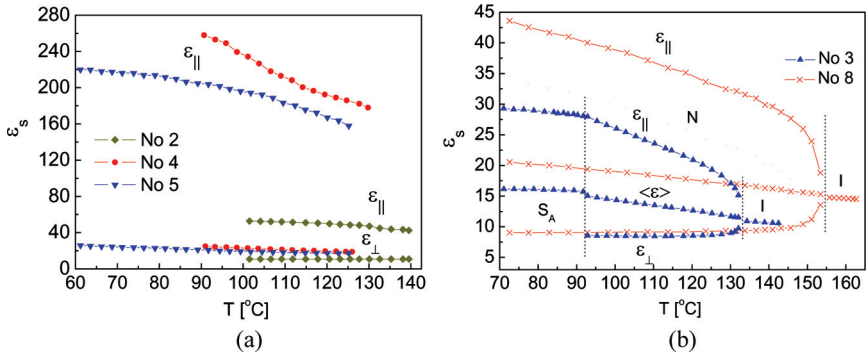

FIGURE 1 The static permittivity tensor components as a function of temperature in the N phase of compound (2), (3), (4) (a), in the LC phases and in the isotropic phase of compound (3) and (8) (b).

of the mixture Base 903 and Base 903 doped with 10% of substance (5) were studied (Figs. 3a and 3b). Assuming additive contributions of both components to the permittivities of the second mixture, the permittivities for pure substance (5) were calculated (Fig. 3c), which yielded results well consistent with other values.

Figure 1b presents the comparison of the static permittivity components as a function of temperature in the S_A, the N and the isotropic phase of compound (3) and in the N phase and the isotropic phase of compound (8). It should be mentioned that only for these two substances the isotropic phase occurs in the temperature range available for the experiment.

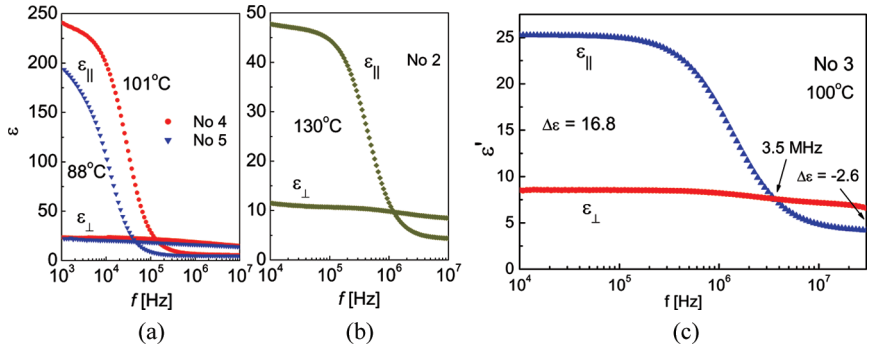

FIGURE 2 Dispersion spectra in the N phase for two orientations of the samples of several substances studied (a and b) with the crossover point marked by an arrow for compound (3) (c).

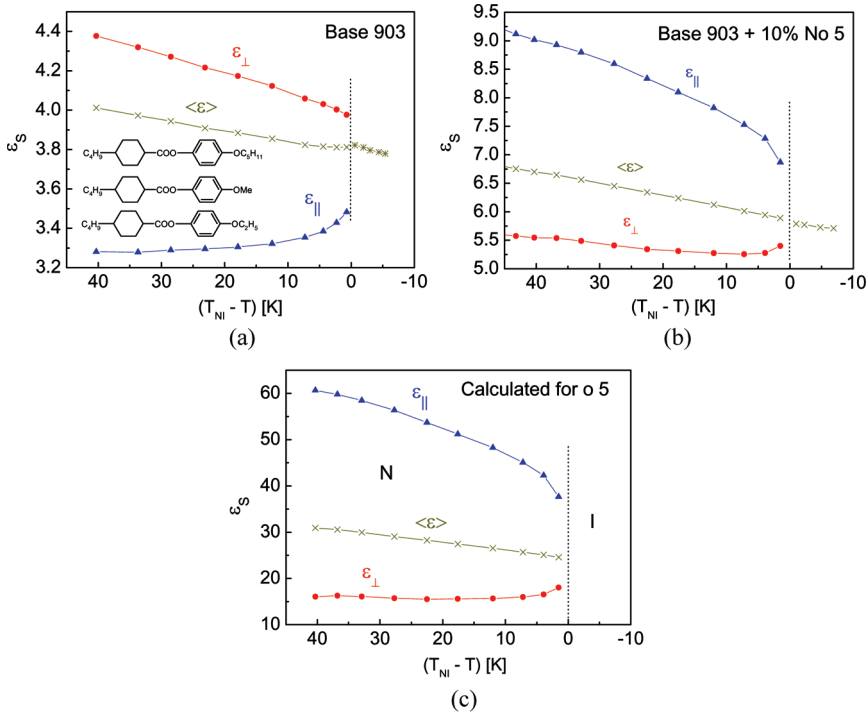

FIGURE 3 Estimation of the static permittivity components for substance (5).

It can be seen from Figure 2 that the dielectric anisotropy changes its sign at MHz frequencies due to dispersion of the parallel component of the dielectric permittivity $\varepsilon'_{\parallel}$ (f), which enables a dual addressing of the LC displays constructed on the basis of such substances. Figure 4 presents the crossover frequency f_{co} for compound (5) as a function of temperature and reversed temperature.

Alignment of compound (3) sample in the S_A phase cooled down from the N phase was saved to some extent, however values of the perpendicular permittivity component $\varepsilon_{\perp}$ increase considerably with lowering temperature (Fig. 1b). Such behaviour may be the result of the dipole-dipole correlations as it was observed for other LC substances [3]. More detailed analysis of this effect could not be carried out because the sample could not be perfectly aligned in the S_A phase either by an available magnetic or an electric field.

The relaxation process connected with the molecular rotation around the short axes, which was visible in the N and the S_A phase,

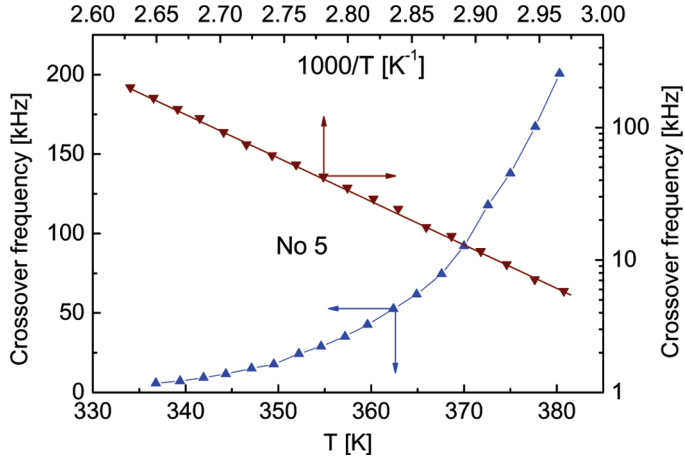

FIGURE 4 The crossover frequency for compound (5) as a function of temperature (lower scale) and reversed temperature (upper scale).

can be described with the Cole-Cole equation:

$$\varepsilon^*(\omega) = \varepsilon'(\omega) - i\varepsilon''(\omega) = \frac{\varepsilon_S - \varepsilon_\infty}{1 + (i\omega\tau)^{1-\alpha}} + \varepsilon_\infty \qquad (1)$$

where ε_S and ε_∞ are the static and the high frequency permittivities, $0 \leq \alpha \leq 1$ describes the distribution of relaxation times τ. For the LC phases α values are close to 0, which indicates that the relaxation process has the monodispersive (Debye-type) character. Examples of the dielectric spectra in the LC phases of compound (3) and (4) are presented in Figure 5 in form of the Cole-Cole plots. Figure 6 shows examples of the Arrhenius plots $\ln\tau$ *versus* $1000/T$ for several substances studied. The calculated activation enthalpies $\Delta H = R(\partial \ln\tau / \partial T^{-1})$, where R is a gas constant, are listed in Table 1.

As it can be seen in Figure 6b, the relaxation times for substance (3) change continuously at the N-S_A phase transition. Similar behaviour was reported for other substances having the N-S_A polymorphism [3–9], however, in case of (3) there is no considerable change in the activation enthalpy values between the N and S_A phases. It seems interesting to add that lowering of the activation enthalpy in the S_A phase was expected due to anisotropic packing effect suggested by Madhusudana *et al.* [6].

The main aim of this work was to analyse the dielectric properties of the substances as related to their chemical structure. With different

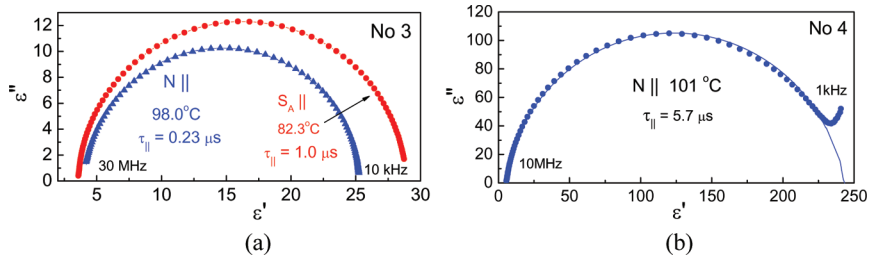

FIGURE 5 The Cole-Cole plots for the N and the S_A phase of compound 3 (a) and for the N phase of compound 4.

cyano and fluoro substituents the molecules have different dipole moments. For all of them the parallel and perpendicular dipole components contribute to the relaxation processes connected with the molecular rotation around the short axis (the low frequency process, *l.f.*) and around the long axis (the high frequency process, *h.f.*). Both processes can be observed in the isotropic phase (see figure 7 for the examples of the dielectric spectra in form of the Cole-Cole plots). The spectra can be therefore described with the superposition of two Cole-Cole equations:

$$\varepsilon^*(\omega) - \varepsilon_\infty = \frac{\delta\varepsilon_{l.f.}}{1 + (i\omega\tau_{l.f.})^{1-\alpha_{l.f.}}} + \frac{\delta\varepsilon_{h.f.}}{1 + (i\omega\tau_{h.f.})^{1-\alpha_{h.f.}}} \qquad (2)$$

where $\delta\varepsilon_{l.f.}$ and $\delta\varepsilon_{h.f.}$ are the dielectric increments for the *l.f.* and *h.f.* processes defined as $\delta\varepsilon = \varepsilon_S - \varepsilon_\infty$. In the case of the isotropic phase

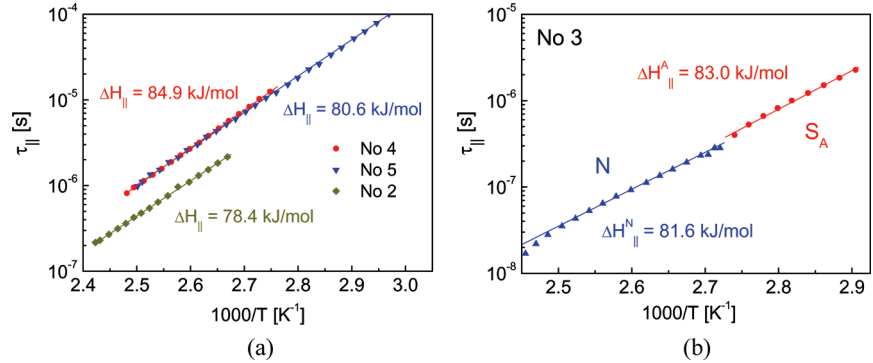

FIGURE 6 The Arrhenius plots in the N phase of compounds (2), (4), (5) (a) and in the N and the S_A phase of compound (3).

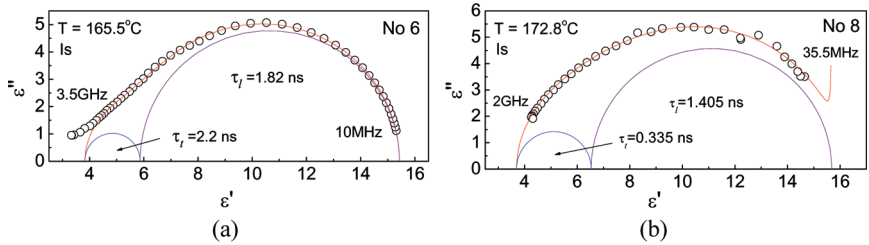

FIGURE 7 The Cole-Cole plot in the isotropic phase of compound (6) (a) and (8) (b).

$\alpha_{l.f.}$ and $\alpha_{h.f.}$ values are also close to 0, indicating the Debye-type character of both relaxation processes.

The axes of rotation are defined as the principal inertia moment axes. They usually differ from the symmetry axes of molecular cores as a result of different lateral attachments to molecular cores or/and conformational changes in terminal alkyl chains. In order to further investigation of the molecular structure the dipole moment μ and the angle β describing its inclination from the long molecular axis were estimated. Similar estimation based on the experimental data for the functional groups which build the LC molecules were reported in [10,11]. However, the so-called GDM method used for reported analysis assumes the planar configuration of a molecule, neglecting its three-dimensional structure. Consequently, it does not yield

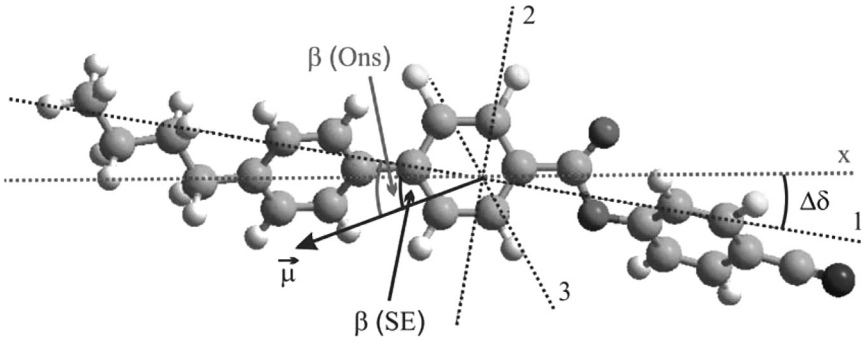

FIGURE 8 The model of compound (6) molecule. The axes of the minimum moment of inertia are marked by 1, 2, and 3. *x*-axis is the *p*-axis of the middle phenyl ring.

TABLE 1 The Chemical Formulas, the Temperatures of Phase Transitions, the Permittivity Components $\varepsilon_{\|}$ and $\varepsilon_{\perp}$ Taken at the Melting Point, the Dielectric Anisotropy $\Delta\varepsilon = \varepsilon_{\|} - \varepsilon_{\perp}$ at Low and High Frequencies, the Crossover Frequency f_{co}, and the Activation Enthalpy ΔH for the Longitudinal Relaxation Process in the Nematic Phase for the Substances Studied

No	Substance	Phase transitions [°C]	$\varepsilon_{\|}$	$\varepsilon_{\perp}$	$\Delta\varepsilon$ *l.f./h.f*	f_{co} [MHz]	ΔH(N) [kJ/mol]
1	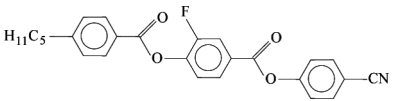	Cr 122 N 228 I	25.5	7.6	17.9–2.46	0.463	77.3
2	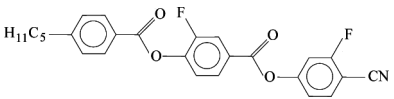	Cr 106 N 198 I	50	11	39–4.3	1.2	78.4
3	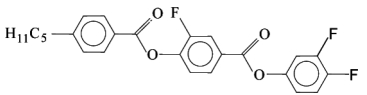	Cr (92.2 SmA) 95 N 133 I	25.3	8.5	16.8–2.6	3.5	81.6 83.0 (SmA)
4	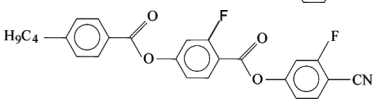	Cr 101 N 202 I	273	23	250–6.6	1.6	84.9
5	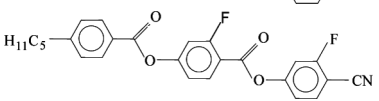	Cr 87 N 200 I	210	23	187–10.9	0.044	80.6
6	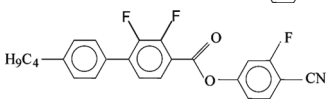	Cr 93 N 158 I	44	13	31–5	1.6	70.2
7	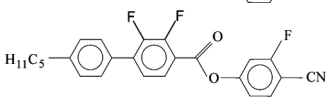	Cr 93.5 N 154.5 I	41.5	11.5	30–4.5	1.5	73.5
8	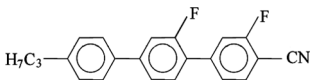	Cr 82.5 N 162 I	42	9	33–3.7	1.2	62

TABLE 2 The Dipole Moment Components and the Angles Between the Dipole Moment and the Molecular Axes as Explained in the Text

Substance No.	μ (SE) [D]	μ_x	μ_y [D]	μ_z	$\Delta\delta$ [°]	β (SE) [°]	β (Ons) [°]
1	7.51	−7.410	−0.841	0.843	5.24	6.43	–
2	8.48	−8.334	−1.502	−0.372	3.37	10.21	–
3	6.78	−6.460	−2.056	−0.087	2.91	17.65	–
4	10.18	−10.250	−1.649	0.106	4.59	9.32	–
5	10.2	−10.067	−1.651	0.149	6.58	9.31	–
6	8.15	−7.552	−2.920	−0.973	9.85	20.98	33.5
7	8.18	−7.778	−2.548	−0.027	8.41	18.14	33.4
8	6.36	−5.979	−2.036	−0.760	2.73	18.67	33.8

satisfactory description of real molecules. In this work the dipole moment of molecules was estimated with the aid of the HyperChem™ Release 7.51 and CS Chem3D Pro with CS MOPAC Pro™ software, based on the semi-empirical AM1 method (a quantum mechanical molecular orbital method with classical empirical parameterization). Table 2 contains the obtained data. The calculation was performed with the reference frame (*x, y, z*) where the *x*-axis was taken as the *p*-axis of the middle phenyl ring (see Fig. 8). All-trans conformation of molecules was assumed. $\Delta\delta$ is the estimated angle between the long axis in the (*x, y, z*) frame and the axis of the minimum moment of inertia (**1**-axis treated as the long molecular axis), β (SE) is the calculated angle between the net dipole moment μ and the long molecular axis.

On the other hand, The angle β (Ons) was calculated for compounds [6–8] taking into account the dielectric increments determined from the analysis of the relaxation spectra measured in the isotropic phase (see Fig. 7 and Eq. (2)). With the aid of well known Onsager equation:

$$\frac{(\varepsilon_s - \varepsilon_\infty)(2\varepsilon_s + \varepsilon_\infty)}{\varepsilon_s(\varepsilon_\infty + 2)^2} = \frac{N_0}{3\varepsilon_0}\frac{\mu^2}{3kT} \tag{3}$$

the ratio $(\mu_t/\mu_l)^2 = \tan\beta$ (Ons) could be estimated, where μ_t and μ_l are the perpendicular and parallel components of the dipole moment. The obtained results are listed in Table 2. As it was expected, the β (Ons) values are comparable to the sum of β (SE) and $\Delta\delta$. It is worth to point out that the calculated and the experimental data seem to agree satisfactorily.

4. CONCLUSIONS

On the basis of a summary of the dielectric properties of eight three ring compounds presented in figures and tables, the following can be concluded:

- Satisfactory estimation of the molecular dipolar structure can be obtained by means of analysis of the experimental results and the theoretical calculations.
- The tensor permittivity components values correlate roughly with the dipole structures of molecules.
- All compounds exhibit large positive dielectric anisotropy at low frequencies and negative anisotropy above the cross-over frequency f_{co}. They can be used to formulation of mixtures for the double addressing displays.
- In all substances the relaxation spectra in the nematic phase can be well described by the Debye equation.
- The activation enthalpy for the end-over-end motion of molecules in the N phase is similar for all compounds.

REFERENCES

[1] Ziobro, D., Kula, P., Dziaduszek, J., Filipowicz, M., Dąbrowski, R., Parka, J., Czub, J., Urban, S., & Wu, S.-T. (2009). Opto-Electronics Review, *17*(1), 16–19.
[2] Gestblom, B., Haase, W., & Wróbel, S. (2003). *Relaxation Phemena*, Springer-Verlag: Berlin, Chapter 1.2, 35.
[3] Urban, S., Czub, J. & Gestblom, B. (2004). *Z. Naturforsch.*, *59a*, 674.
[4] Urban, S. & Würflinger, A. (2003). *Relaxation Phemena*, Haase, W. & Wróbel, S. (Eds.), Springer-Verlag: Berlin, Chapter 4.2, 181.
[5] Wacrenier, J. M., Druon, C., & Lippens, D. (1981). *Mol. Phys.*, *43*, 97.
[6] Madhusudana, N. V., Brikanta, B. S., & Subramanya Raj Urs, M. (1984). *Mol. Cryst. Liq. Cryst.*, *108*, 19; Srikanta, S. & Madhusudana, N. V. (1984). *Mol. Cryst. Liq. Cryst.*, *108*, 39.
[7] Urban, S., Novotna, E., Kresse, H., & Dąbrowski, R. (1995). *Mol. Cryst. Liq. Cryst.*, *262*, 257.
[8] Urban, S., Kresse, H., & Dąbrowski, R. (1997). *Z. Naturforsch.*, *52a*, 403.
[9] Czub, J., Pawlus, S., Sekuła, M., Urban, S., Würflinger, A., & Dąbrowski, R. (2003). *Z. Naturforsch.*, *58a*, 333.
[10] Minkin, W. I., Osipov, O. A., & Zhdanov, Yu. A. (1970). *Dipole Moments in Organic Chemistry*, Plenum Press: New York.
[11] Exner, O. (1975). *Dipole Moments in Organic Chemistry*, Georg Thieme: Stuttgart.